Interaction of Energetic Ions with Inhomogeneous Solids

M. Bode, A. Ourmazd, and J. Cunningham
AT&T Bell Laboratories, Holmdel, New Jersey 07733

M. Hong
AT&T Bell Laboratories, Murray Hill, New Jersey 07974
(Received 26 April 1991)

We use quantitative chemical mapping and statistical analysis to explore the microscopic consequences of the passage of energetic ions through AlAs/GaAs multilayers. We thus quantitatively characterize and microscopically identify the damage cascades produced by individual 320-keV Ga^+ ions. Our results reveal a strong drift of the damage in an applied electric field, indicating the defects to be charged. We exploit this effect to show that the defects produced by the passage of energetic ions may be microscopically steered in a solid.

PACS numbers: 61.80.Jh, 61.16.Di, 73.40.Kp

A gedanken experiment to investigate ion-solid interactions at their most fundamental level might consist of imaging the atomic consequences of the passage of individual energetic ions through a solid. Here we describe how this may be approached in practice. An ion implanted into a multilayer can cause intermixing at each interface, in the same way that cosmic radiation can activate the grains of a stack of photographic emulsion layers. We use stacks of AlAs/GaAs interfaces to record the passage of 320-keV Ga^+ ions through multilayers at 77 K. In analogy with photography, the "development" process consists of imaging the atomic intermixing at each interface by quantitative chemical mapping [1-3]. This electron-microscopic method measures the composition of individual atomic columns in the vicinity of an interface.

Our results can be summarized as follows. First, the damage track produced by the passage of a single ion consists of a heavily damaged core ~ 15 Å in diameter, broadening an initially 2.7-Å-wide AlAs/GaAs interface in its path to a width of ~ 20 Å. This broadening is substantially larger than expected on kinematic grounds alone. Second, the defects generated by the primary ions drift to and accumulate at nearby interfaces. Third, the direction in which the defects drift can be controlled by the application of an electric field. Our observations elucidate the nature of single-ion–solid interactions, and offer the possibility of their control at the atomic level.

The multilayers used in our experiments consisted of twenty periods of (50 Å AlAs–50 Å GaAs), sandwiched between a 2000-Å GaAs buffer layer, and a 250- or 450-Å GaAs cap, grown by molecular-beam epitaxy on semi-insulating (100) GaAs. The buffer and cap layers were either nominally undoped (in fact, p type with a carrier concentration $< 10^{15}$ cm^{-3}) or doped to produce p-i-n or n-i-p structures with the multilayers forming the "intrinsic" region in each case. 320-keV Ga^+ ions were implanted at ≈ 77 K, to doses in the range 5×10^{12}–5×10^{13}/cm^2, at a rate of 10^{10} ions/s. Cross-sectional samples were subsequently mechanically polished and chemically etched to perforation for electron-microscopic examination. Our thinning procedure requires treatment at temperatures of up to 150 °C, leaving only the heavily damaged cores that are stable at this temperature [4]. Quantitative chemical maps of the interfaces were obtained before and after ion implantation in 100–150-Å-thick regions of samples, as previously described [1-3]. We have already established that GaAs/AlAs interfaces are not affected by the imaging process itself [3].

Figure 1 is a chemical lattice image of an unimplanted GaAs layer between its adjacent AlAs neighbors. Using vector pattern recognition [1-3], we extract from such images the composition of individual atomic columns in the vicinity of the interface, and the confidence level for each measurement. Figure 1 also shows composition profiles across the "top" (AlAs on GaAs) and "bottom" (GaAs on AlAs) interfaces, obtained by averaging the composition over a number of atomic columns lying on individual planes parallel to the interface. The interface width is quantified in terms of the best fit of an error function to the experimental data. In our samples, the top (AlAs on GaAs) and bottom (GaAs on AlAs) interfaces have similar widths to within $\sim 10\%$. Figure 2 is a chemical lattice image of a top (AlAs on GaAs) interface at a depth of 1100 Å from the surface (i.e., in the middle of the ion range) after implantation to a dose of 5×10^{12}

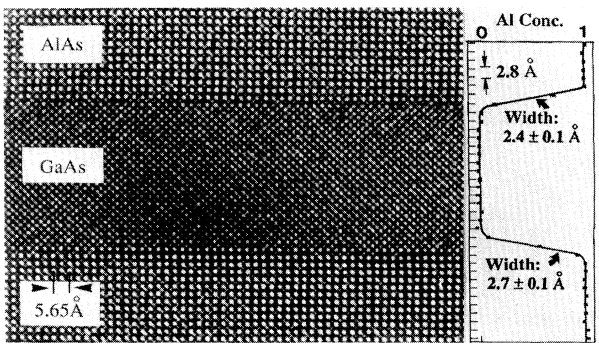

FIG. 1. Chemical lattice image and composition profiles for two AlAs/GaAs interfaces. Each data point represents the composition of a 1-μm segment of an atomic plane parallel to the interface.

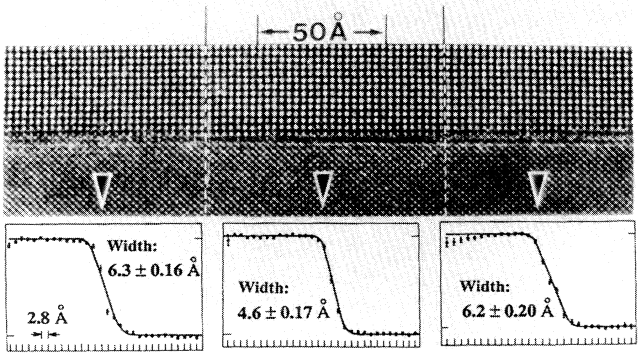

FIG. 2. Chemical lattice image of an AlAs on GaAs interface, implanted with 5×10^{12} ions/cm^2. The chemical profiles, obtained by averaging over 50-Å segments of planes parallel to the interface, show substantial variation in the GaAs→AlAs transition width.

ions/cm^2 [1 ion/(2000 Å^2)]. Composition profiles, obtained by averaging the composition over adjacent 50-Å segments of planes parallel to the interface, now reveal substantial variation in the interface width, not present in the unimplanted sample. The broadening of the interfacial profile is most pronounced in the middle of the ion range, becoming undetectable in the near-surface and past-end-of-range regions.

We now describe how such data may be analyzed to extract the characteristics of the damage tracks produced by individual ions. In a sample of thickness t, we consider the fates of narrow strips of width s, lying in the interfacial plane and crossing one or more damage tracks (Fig. 3). Assume for the moment that the entire interface has the same compositional width (i.e., that the interface consists of a large number of identical strips of compositional widths L_u before implantation), and that the effect of implantation is to produce identical, well separated damage cylinders of diameter d, within each of which the interface width is broadened to L_i. Consider a strip lying in the path of n ions. The interfacial width measured in our experiments is a weighted average over

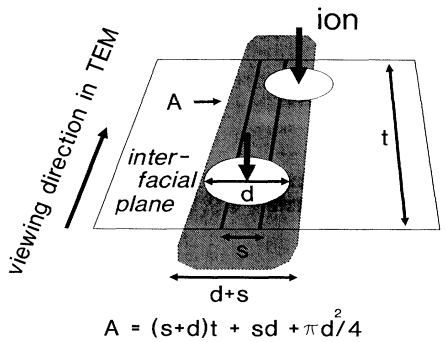

FIG. 3. Schematic representation of the effect of implantation on a narrow strip s, lying in the interfacial plane of a sample of thickness t. Any ion piercing the area A affects the strip s. Area A depends on the diameter d of the damage track.

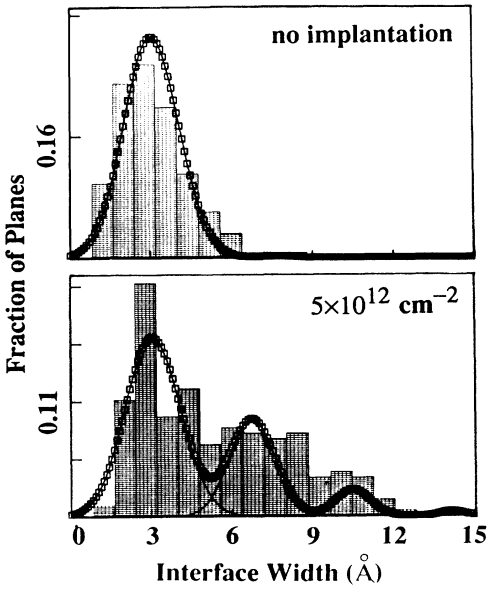

FIG. 4. Histogram of transition widths from AlAs to GaAs for (AlAs on GaAs) interfaces of the multilayer, implanted with 320-keV Ga^+ ions at 77 K. The curve is the fitted plot of $P(n)$ vs $L(n)$. The diameter of the damage cascade, the ion dose μ, and the amount of intermixing caused by a single ion L_i were the fitting parameters. (The dose is a fit parameter because, on average, an ion need not create exactly one damage track at each interface. The fitted dose and the actual dose agree to within 25%.)

the length of the strip, because we view the strips "endon." In the low-dose limit (i.e., without overlap of damage cascades), this average interfacial width is given by $L_n=(1/t)[ndL_i+(t-nd)L_u]$. Since the arrival of the ions is governed by Poisson statistics, the probability that a strip of width s lies in the damage cylinder of n ions is given by $P_n=[(\mu A)^n/n!]\exp(-\mu A)$, where μ is the ion dose. Thus, starting with N virgin strips, the implantation process divides these strips into sets, each containing NP_n members characterized by an interfacial width L_n. In reality, the unimplanted strips are characterized not by a unique compositional width L_u, but by a Gaussian centered at L_u, and the implanted interface is characterized by a set of Gaussians each centered at L_n, with relative heights given by P_n.

In our experiments, each strip is one atomic plane (2.8 Å) wide. Figure 4 shows typical histograms of the compositional widths for a large number of such strips in an unimplanted sample, and for samples implanted at 5×10^{12} cm^{-2}. Such histograms are essentially plots of P_n vs L_n. Deducing the initial Gaussian distribution from the unimplanted samples and the sample thicknesses from our lattice images, we have fitted histograms for six samples, each implanted and analyzed separately to obtain the characteristics of the individual damage tracks (Fig. 4). All the fits at a given dose yield a consistent set of parameters. (For lack of space, we present results for only

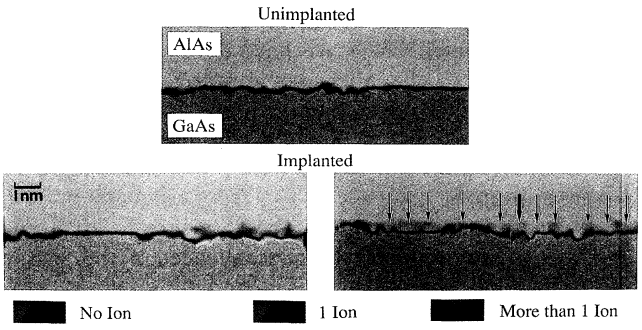

FIG. 5. Result of a computer search for damage tracks in an unimplanted sample and two typical implanted samples. The color code represents the interfacial width, with black, red, and green designating widths characteristic of the regions of the interface pierced by no ions, one ion, and more than one ion, respectively.

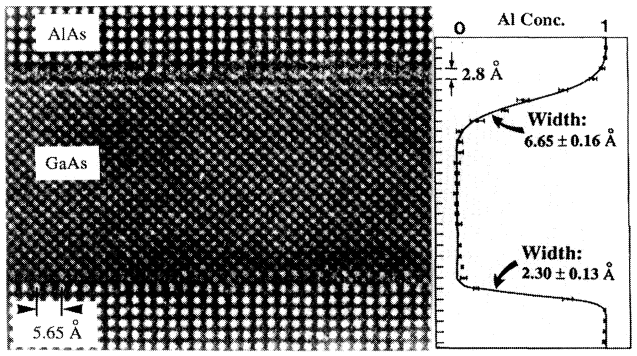

FIG. 6. Chemical lattice image of an AlAs/GaAs/AlAs period, implanted with 5×10^{12} ions/cm^2. The "top" interface (AlAs on GaAs) shows clear signs of intermixing, while the "bottom" interface (GaAs on AlAs) is not affected.

one dose. The dose dependence of our observations, to be discussed elsewhere, allows us to conclude that we are characterizing the damage tracks created by individual ions.) At a dose of 5×10^{12} ions/cm^2, the damage track consists of a core $\sim$15 Å in diameter, within which the interfacial composition width is increased from the initial value of 2.7 to $\sim$20 Å. This is substantially larger than the intermixing expected from kinematic (TRIM [5]) simulations ($\sim$5 Å). The deduced interfacial composition width L_n and the widths of the damage cascades act as microscopic signatures, allowing us to identify regions affected by the passage of n ions ($n=0,1,2,\ldots$). Figure 5 shows the color-coded results of a computer search through three chemical lattice images, where the black, red, and green segments represent regions pierced by no ions, one ion, and two or more ions, respectively. These images represent microscopic records of the passage of individual ions through the sample.

We now show that there are remarkable differences between the behavior of adjacent interfaces [6]. Figure 6 shows neighboring top (AlAs on GaAs) and bottom (GaAs on AlAs) interfaces after implantation to a dose of 5×10^{12} ions/cm^2. The composition profiles (Fig. 6) and interface-width histograms (not shown) extracted from such images clearly establish that the top interface is substantially broadened by implantation, but the bottom interface is left practically unaltered. Implanting 320-keV Ga^+ ions into our 2000-Å-thick multilayer is roughly analogous to firing a bullet through a telephone book. We find that only every other sheet has developed a hole. This remarkable effect, totally unexpected on kinematic grounds [5], is due to, and can be controlled by means of, an electric field. In the sample we have so far considered (held at 77 K during implantation), the Fermi level is most likely pinned at midgap at the surface of the GaAs cap layer, and close to the valence band at 3000 Å from the surface, placing the multilayer in an electric field. We now show that the large intermixing asymmetry observed at the top and bottom interfaces is due to the drift of the implantation damage in the electric field to the (AlAs on GaAs) interfaces, where it is trapped. As described by Tersoff [7], we believe this trapping is due to the discontinuities in the band structure and the formation enthalpies of the defects involved. Experimental proof of the influence of the electric field rests on our ability to reverse the asymmetry of the intermixing between the top and bottom interfaces by reversing the electric field. The field reversal is achieved by embedding "intrinsic" multilayers in *p-i-n* and *n-i-p* structures, and comparing the intermixing at the "top" and "bottom" interfaces. In Fig. 7, we compare the histograms obtained from the *p-i-n* and *n-i-p* structures. The clear reversal of the asymmetry in intermixing firmly establishes the strong influence of the electric field in determining the location of the defect agglomerates responsible for the intermixing.

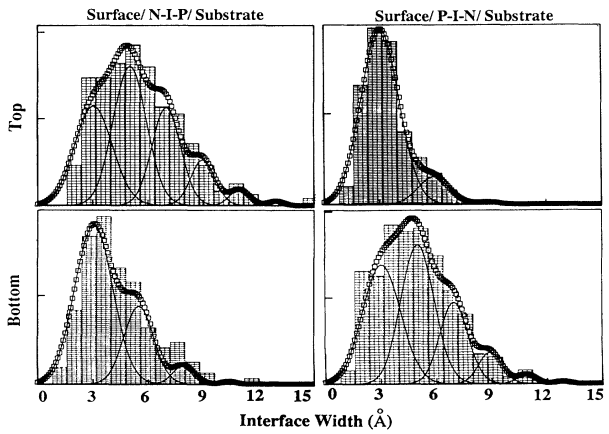

FIG. 7. Histogram of interface widths for "top" and "bottom" interfaces embedded in *p-i-n* and *n-i-p* structures. In the *n-i-p* structure the top interface (AlAs on GaAs) is strongly intermixed, while in the *p-i-n* structure, the bottom interface (GaAs on AlAs) is strongly intermixed.

We now address the question of tracking an individual ion through many interfaces. To identify a single ion at one interface requires the damaged segment created by the ion to be flanked by, say, ~8-Å segments of undamaged interface on either side. The probability to observe such an event is ~1.6%. To identify a single track through two interfaces requires that the area at the second interface through which the designated ion may pass should not be pierced by other ions. This yields a probability of ~0.17% for detecting the damage left by a single ion at two successive (AlAs on GaAs) interfaces in our experiments [8]. In view of this exceedingly small value, we have not attempted to identify the damage track left by a single ion at more than one interface. However, it is now straightforward to design experiments in which such tracking should be possible.

We now discuss the nature of the defects giving rise to our observations. The strong response of the defects to an applied electric field clearly shows that the defects produced by our implantation process are charged. However, quantitative chemical mapping is not spectroscopic. In III-V materials, it simply measures the total projected potential of a group-III atomic column relative to its group-V neighbors. The increases in the interfacial width that we observe can thus be due to Ga→ Al interchanges, or to agglomeration of point defects such as vacancies and interstitials. In agreement with previous work [9,10], we observe extrinsic extended defects (loops) when our implanted samples are annealed at 600 °C for 2 h, indicating condensation of interstitial point defects in the interior of the GaAs. However, this does not unequivocally establish that interstitials are responsible for the effects we observe. Also, since the ionization and formation enthalpies for point defects in GaAs and AlAs are not available, we are not able to deduce the nature of the defects from their response to the electric field [7].

We now discuss the wider implications of our results. Modern electronic devices are highly inhomogeneous structures with submicron dimensions, whose fabrication often requires the introduction of very small numbers of impurities into predetermined areas of the device. Our results offer the tantalizing prospect of steering point defects in a lattice by means of applied electric fields. For example, one can envisage using internal electric fields to steer implantation damage to preordained "trash bin" sites not critical to the performance of the device. From a scientific point of view, we have developed a quantitative approach to the microscopic study of ion-solid interactions. This is conceptually similar to the use of photographic emulsions in high-energy physics, and may prove equally powerful in elucidating the fundamentals of ion implantation.

In conclusion, we have described a means for determining, at the atomic level, the consequences of the passage of individual energetic ions through inhomogeneous solids. The implantation of ions into GaAs/AlAs multilayers produces charged defects, which respond to, and can be controlled by, electric fields. We may have thus discovered a means for the exploration and control of ion implantation at the microscopic level.

We acknowledge valuable discussions with F. H. Baumann, A. Bourret, W. L. Brown, D. J. Eaglesham, L. C. Feldman, R. E. Howard, and J. M. Poate, and are grateful to J. A. Rentschler for expert technical assistance.

[1] A. Ourmazd, D. W. Taylor, J. Cunningham, and C. W. Tu, Phys. Rev. Lett. **62**, 933 (1989).
[2] A. Ourmazd, D. W. Taylor, M. Bode, and Y. Kim, Science **246**, 1571 (1989).
[3] A. Ourmazd, F. H. Baumann, M. Bode, and Y. Kim, Ultramicroscopy **34**, 237 (1990).
[4] J. S. Vetrano, M. W. Bench, I. M. Robertson, and M. A. Kirk, Met. Trans. A **20A**, 2673 (1989).
[5] J. P. Biersack, Nucl. Instrum. Methods Phys. Res., Sect. B **19**, 32 (1987).
[6] M. Bode, A. Ourmazd, J. A. Rentschler, M. Hong, L. C. Feldman, and J. P. Mannaerts, Mater. Res. Soc. Symp. Proc. **157**, 197 (1990).
[7] J. Tersoff, Phys. Rev. Lett. **65**, 887 (1990).
[8] This estimate relies on kinematic simulations of damage tracks by TRIM [5] which show the angular distribution of the ion tracks to be nearly Gaussian with widths σ of 25° and 35° at depths of 450 and 1100 Å, respectively.
[9] J. Ralston, G. W. Wicks, L. F. Eastman, B. C. deCooman, and C. B. Carter, J. Appl. Phys. **59**, 120 (1986).
[10] B. C. DeCooman, C. B. Carter and J. R. Ralston, Proc. SPIE **797**, 185 (1987).

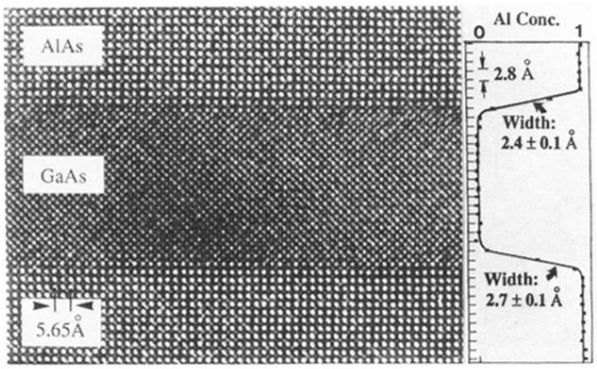

FIG. 1. Chemical lattice image and composition profiles for two AlAs/GaAs interfaces. Each data point represents the composition of a 1-μm segment of an atomic plane parallel to the interface.

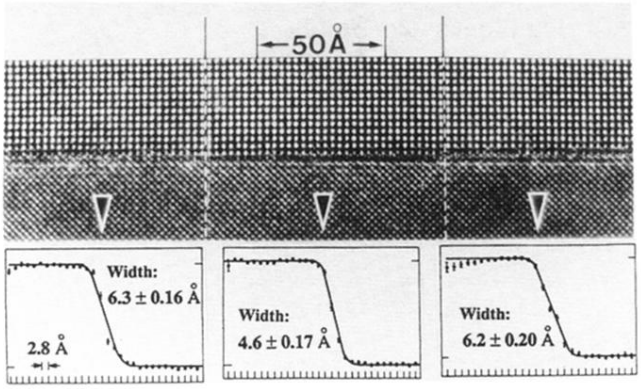

FIG. 2. Chemical lattice image of an AlAs on GaAs interface, implanted with 5×10^{12} ions/cm^2. The chemical profiles, obtained by averaging over 50-Å segments of planes parallel to the interface, show substantial variation in the GaAs→AlAs transition width.

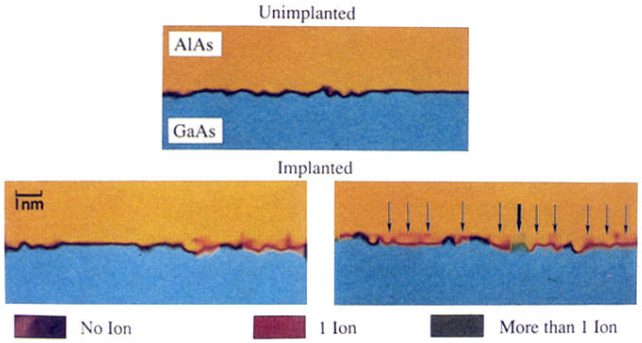

FIG. 5. Result of a computer search for damage tracks in an unimplanted sample and two typical implanted samples. The color code represents the interfacial width, with black, red, and green designating widths characteristic of the regions of the interface pierced by no ions, one ion, and more than one ion, respectively.

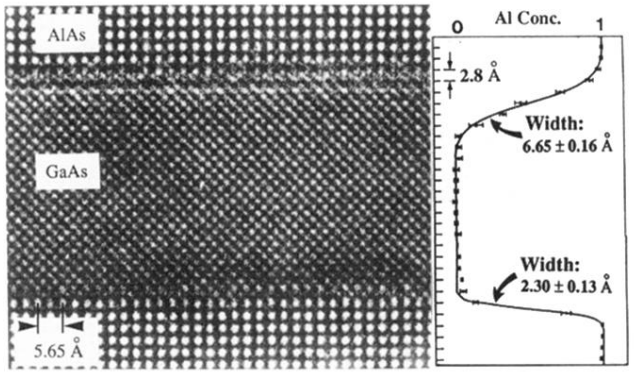

FIG. 6. Chemical lattice image of an AlAs/GaAs/AlAs period, implanted with 5×10^{12} ions/cm^2. The "top" interface (AlAs on GaAs) shows clear signs of intermixing, while the "bottom" interface (GaAs on AlAs) is not affected.